



# C–H⋯Pt(II) interaction-controlled self-assembly and photophysics of chiral bis(pyrrol-2-ylmethyleamino)cyclohexane platinum(II) complexes

Xu-Feng Shan, Deng-Hui Wang, Chen-Ho Tung, Li-Zhu Wu\*

Laboratory of Organic Optoelectronic Functional Materials and Molecular Engineering, Technical Institute of Physics Chemistry and Graduate University, the Chinese Academy of Sciences, Beijing 100190, PR China

## ARTICLE INFO

### Article history:

Received 6 November 2007

Received in revised form 19 March 2008

Accepted 25 March 2008

Available online 28 March 2008

## ABSTRACT

Reaction of (*R,R*)-(–)- and (*S,S*)-(+)-1,2-bis(pyrrol-2-ylmethyleamino)cyclohexane with  $K_2PtCl_4$  afforded chiral, neutral platinum(II) Schiff base complexes of (*R,R*)-**PtL** and (*S,S*)-**PtL** with high yields. The rare C–H⋯Pt(II) intermolecular interaction was found to show considerable strength and directionality for controlling *M* and *P* helical supramolecular architectures of (*R,R*)-**PtL** and (*S,S*)-**PtL**, respectively, in crystal lattices. More importantly, the open square-planar geometry of platinum(II) complexes allows axial C–H⋯Pt(II) interaction, resulting in the  $^3(\pi\pi^*)$  excited state with some mixing of the Pt(II) metal character observed both in concentrated solutions and in the solid state at room temperature.

© 2008 Elsevier Ltd. All rights reserved.

## 1. Introduction

Platinum(II) complexes with  $d^8$  electronic configuration have been recently demonstrated to be promising in material science.<sup>1–7</sup> It is generally accepted<sup>1–4</sup> that when two platinum(II) units are in close proximity, metal–metal and/or ligand–ligand interactions result in the metal–metal-to-ligand charge transfer (MMLCT:  $[d\sigma^* \rightarrow \pi^*]$ ) and/or excimeric ligand-to-ligand ( $\pi \rightarrow \pi^*$ ) excited states. Unusual colors and lower energy emissions relative to the mononuclear species are often the results of metal–metal and ligand–ligand interactions. Subtle manipulation of the intermolecular interactions can alter the crystalline structures and photoluminescence properties remarkably.

C–H⋯M (M: metal) interaction was initially postulated in the literature<sup>8</sup> and has become increasing evident that metals can directly participate in the C–H⋯M three-center interaction.<sup>8–10</sup> Very recently, C–H⋯M interactions were found to be responsible for the facile formation of homochiral helices of the chiral, neutral, mononuclear (*R,R*)- and/or (*S,S*)-bis(pyrrol-2-ylmethyleamino)-cyclohexane complexes in crystal lattices.<sup>10d–f</sup> Notably, the use of pyrrol-2-yl Schiff base avoided counterion coordination<sup>10–12</sup> and thereby achieved exclusive coordination of the tetradentate ligand to the metal center.

Interest in photophysics and photochemistry of platinum(II) complexes<sup>6,7</sup> prompts us to investigate bis(pyrrol-2-ylmethyleamino)cyclohexane platinum(II) complexes. Since the excited state energies are susceptible to the metal–metal and/or ligand–

ligand distances,<sup>1</sup> bis(pyrrol-2-ylmethyleamino)cyclohexane platinum(II) complexes here are expected to model the excited state energy of C–H⋯M interaction-driven homochiral *M* and *P* helices, which have not yet been noted in neutral platinum(II) monomeric complexes. In the present work, we report that the chirality of the neutral, mononuclear, square-planar platinum(II) complexes (*R,R*)-**PtL** and (*S,S*)-**PtL** extends over the whole supramolecular architectures by the intermolecular C–H⋯Pt(II) interaction forming the homochiral left-handed (*M*) and right-handed (*P*) helices in the crystal packing. More importantly, the open square-planar geometry of platinum(II) complexes allows axial C–H⋯Pt(II) interaction, and as a result, the  $^3(\pi\pi^*)$  excited state with some mixing of the Pt(II) metal character is observed both in concentrated solutions and in the solid state at room temperature.

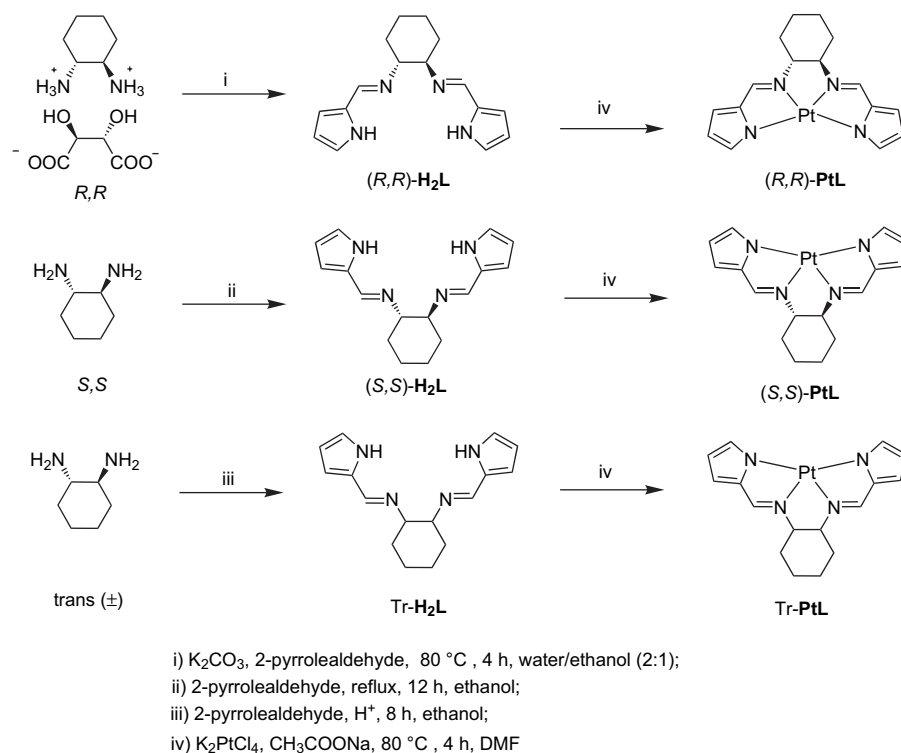
## 2. Results and discussion

### 2.1. Syntheses and characterization

In the presence of  $CH_3COONa$ , the two enantiomeric ligands of (*R,R*)-(–)- and (*S,S*)-(+)-1,2-bis(pyrrol-2-ylmethyleamino)cyclohexane, prepared according to the literature method,<sup>10e</sup> were reacted with  $K_2PtCl_4$  to afford neutral mononuclear complexes (*R,R*)-**PtL** and (*S,S*)-**PtL** with yields of 79 and 78%, respectively, in DMF solution (Scheme 1). The racemic complex Tr-**PtL** was also synthesized for comparison. Combined with  $^1H$  and  $^{13}C$  NMR spectroscopies, FAB-MS spectrometry, and satisfactory elemental analyses, the identity of complexes was determined to be a monomeric complex with a metal-to-ligand ratio of 1:1. The neutral

\* Corresponding author. Tel./fax: +86 10 82543580.

E-mail address: [lzwu@mail.ipc.ac.cn](mailto:lzwu@mail.ipc.ac.cn) (L.-Z. Wu).



**Scheme 1.** Synthetic routes of (R,R)-PtL, (S,S)-PtL, and Tr-PtL.

complexes are stable in air at room temperature and are soluble in common organic solvents.

High-performance liquid chromatographic analysis was performed to examine the optical purity of (R,R)-PtL and (S,S)-PtL. Evidently, only one product peak was present when respective (R,R)-PtL and (S,S)-PtL were analyzed by HPLC on a CHIRALPAK<sup>®</sup> IA column (Daicel Chemical Industries, Ltd.,  $1.0 \times 25$  cm; eluent: ethanol; flow rate:  $2.0 \text{ mL/min}$ ; UV detection at  $388 \text{ nm}$ ;  $25^\circ\text{C}$ ) (Fig. 1). In contrast, the racemic complex of Tr-PtL was resolved into two identical peaks in magnitude, corresponding to that observed in (R,R)-PtL and (S,S)-PtL, respectively. Furthermore, the isolated two enantiomers show near mirror image behavior in the circular

dichroism (CD) spectra, while the absorption spectra are not distinguishable from each other (see below).

## 2.2. Intermolecular C–H $\cdots$ Pt(II) interaction-controlled homochiral supramolecular M and P helices in the crystal packing

Single crystals of (R,R)-PtL, (S,S)-PtL, and Tr-PtL were obtained by slow evaporation of the mixture of  $\text{CH}_2\text{Cl}_2$ – $\text{CH}_3\text{OH}$  solution. Orange single crystals as needles were used for data collection on a Bruker Smart 1000 X-ray diffractometer with Mo  $\text{K}\alpha$  radiation. The crystals of (R,R)-PtL and (S,S)-PtL belong to the monoclinic crystal system and  $P2_1$  space group, while Tr-PtL belongs to the monoclinic crystal system and  $P2_1/c$  space group (Table 1). Figure 2 shows the two neutral mononuclear (R,R)-PtL and (S,S)-PtL complexes. Obviously, the Pt(II) center is four-coordinated to four N atoms from pyrrol-2-yl-cyclohexenediamine Schiff base unit and has a small deviation from the square-planar coordination geometry.

The rare intermolecular C–H $\cdots$ M interaction was found in the molecular packing of (R,R)-PtL and (S,S)-PtL, similar to that observed in nickel(II) complexes.<sup>10e</sup> Each ligand uses its hydrogen atoms to bind the platinum(II) center of the others. Since the two pyrrol-2-yl-diamino units of the same ligand adopt a cis-conformation and the C–N(imine) bonds in the rigid *trans*-1,2-cyclohexyl moiety are arranged reciprocally, the unit cell contains three different C–H $\cdots$ Pt(II) intermolecular interactions in the crystal packing (Fig. 2). The intermolecular contacts of  $2.910 \text{ \AA}$  at  $\text{C43B} \cdots \text{H43B} \cdots \text{Pt1B}$ ,  $2.988 \text{ \AA}$  at  $\text{C6CA} \cdots \text{H6CA} \cdots \text{Pt3B}$ , and  $3.066 \text{ \AA}$  at  $\text{C11A} \cdots \text{H11A} \cdots \text{Pt3B}$  with the C–H $\cdots$ Pt(II) angle of  $145.6^\circ$ ,  $145.5^\circ$  and  $167.1^\circ$  (Table 2), respectively, lead to the formation of helical assemblies with different pitches in the helix of (R,R)-PtL. Four complexes fragments form one helix with screw-pitch of  $17.109 \text{ \AA}$ . Obviously, the turn required to generate a perfect periodic self-assembly of (R,R)-PtL in a helical fashion is induced by the chirality of the building block

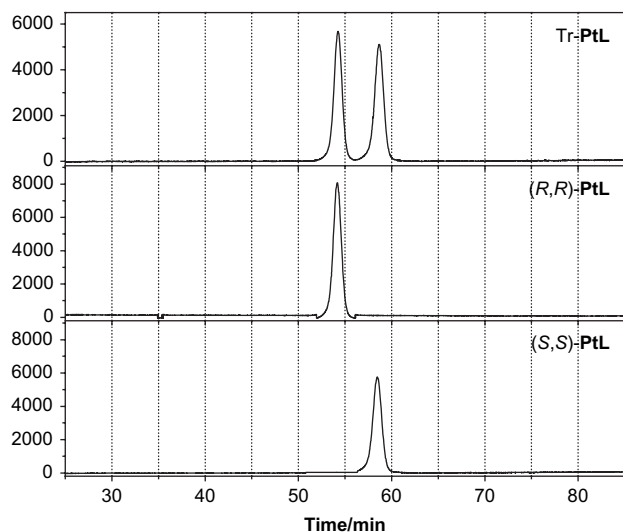


**Figure 1.** HPLC traces of (R,R)-PtL, (S,S)-PtL, and Tr-PtL (eluted with ethanol with flow rate of  $2.0 \text{ mL min}^{-1}$  and monitored at  $\lambda = 388 \text{ nm}$ ).

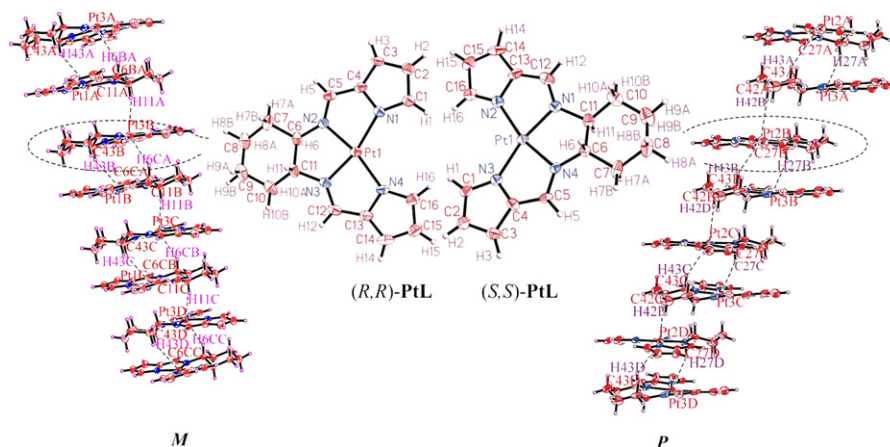
**Table 1**The crystal data of (*R,R*)-**PtL**, (*S,S*)-**PtL**, and Tr-**PtL**.

	Compound		
	( <i>R,R</i> )- <b>PtL</b>	( <i>S,S</i> )- <b>PtL</b>	Tr- <b>PtL</b>
Empirical formula	C <sub>16</sub> H <sub>18</sub> N <sub>4</sub> Pt	C <sub>16</sub> H <sub>18</sub> N <sub>4</sub> Pt	C <sub>16</sub> H <sub>18</sub> N <sub>4</sub> Pt
Formula weight	461.43	461.43	461.43
Crystal system, space group	Monoclinic, <i>P</i> 2 <sub>1</sub>	Monoclinic, <i>P</i> 2 <sub>1</sub>	Monoclinic, <i>P</i> 2 <sub>1</sub> / <i>c</i>
Unit cell dimensions			
<i>a</i> /Å	18.1252(16)	18.045(8)	21.187(5)
<i>b</i> /Å	8.5546(8)	8.566(4)	8.620(2)
<i>c</i> /Å	21.2974(19)	21.230(9)	17.861(4)
$\alpha$ /°	90	90	90
$\beta$ /°	112.5760(10)	112.587(5)	112.704(3)
$\gamma$ /°	90	90	90
Volume/Å <sup>3</sup>	3049.2(5)	3030(2)	3009.3(12)
<i>Z</i> , <i>D</i> <sub>c</sub> /g cm <sup>−3</sup>	8, 2.010	8, 2.023	8, 2.037
Absorption coefficient/mm <sup>−1</sup>	9.202	9.261	9.324
<i>F</i> (000)	1760	1760	1760
Crystal size/mm <sup>3</sup>	0.24×0.20×0.12	0.49×0.18×0.10	0.30×0.20×0.15
$\theta$ Range for data collection/°	1.04–26.39	1.04–25.10	1.04–25.03
Limiting indices	−22≤ <i>h</i> ≤20 −10≤ <i>k</i> ≤10 −18≤ <i>l</i> ≤26	−21≤ <i>h</i> ≤21 −10≤ <i>k</i> ≤10 −25≤ <i>l</i> ≤22	−25≤ <i>h</i> ≤19 −9≤ <i>k</i> ≤10 −15≤ <i>l</i> ≤21
Reflections collected/unique	17,303/11,774 [ <i>R</i> (int)=0.0283]	14,989/9941 [ <i>R</i> (int)=0.0442]	12,212/5308 [ <i>R</i> (int)=0.0356]
Completeness to $\theta$	99.7%	99.3%	99.8%
Max. and min. transmission	0.4047 and 0.2161	0.4578 and 0.0927	0.3352 and 0.1663
Data/restraints/parameters	11,774/1/757	9941/13/759	5308/0/379
Goodness-of-fit on <i>F</i> <sup>2</sup>	1.013	1.008	1.042
Final <i>R</i> indices [ <i>I</i> > 2 $\sigma$ ( <i>I</i> )]	<i>R</i> 1=0.0398, <i>wR</i> 2=0.1003	<i>R</i> 1=0.0504, <i>wR</i> 2=0.1336	<i>R</i> 1=0.0380, <i>wR</i> 2=0.0952
<i>R</i> indices (all data)	<i>R</i> 1=0.0597, <i>wR</i> 2=0.1139	<i>R</i> 1=0.0606, <i>wR</i> 2=0.1443	<i>R</i> 1=0.0487, <i>wR</i> 2=0.1000
Absolute structure parameter	0.014(14)	0.030(16)	—
Largest diff. peak and hole/e Å <sup>−3</sup>	1.779 and −1.567	2.122 and −3.105	2.059 and −1.408

coupled with the strong C–H⋯Pt(II) interactions. An *M* handedness can be clearly assigned to complexes (*R,R*)-**PtL** when viewed along the *b* axis. This local chirality at the molecular level translates throughout the crystal into the formation of only left-handed (*M*) helices at the supramolecular level. The path of the helix can be easily traced by following the hydrogen bonds counterclockwise around the screw axis of the helix. Similar self-assembling pattern exists in the crystal packing of (*S,S*)-**PtL**. The only difference is the presence of opposite direction, in which the intermolecular C–H⋯Pt(II) interaction shows clockwise around the screw axis to give a right-handed (*P*) helix. In contrast, the self-assembling manner present in racemic Tr-**PtL** is different from those in (*R,R*)-**PtL** and (*S,S*)-**PtL**. Two molecules of (*R,R*)-**PtL** and (*S,S*)-**PtL** are interacted with each other in one unit cell via intermolecular C–H⋯Pt(II) interactions (Fig. 3). Only one H atom from 1,2-cyclohexyl in one molecule of Tr-**PtL** is bound to Pt(II) center of the other, resulting in the assembling picture far from those of (*R,R*)-**PtL** and (*S,S*)-**PtL** helices.

### 2.3. Photophysical properties

Such homochiral *M* and *P* helices of (*R,R*)-**PtL** and (*S,S*)-**PtL** in the crystal packing prompt an investigation of the photophysical properties. Figure 4 shows the UV–vis absorption and circular dichromism (CD) spectra of the complexes studied in this work. All the complexes exhibit intense vibronic absorption bands at  $\lambda < 400$  nm ( $\epsilon = 1.3\text{--}1.6 \times 10^4$  dm<sup>3</sup> mol<sup>−1</sup> cm<sup>−1</sup>) and a moderately intense low-energy absorption bands in the range of 400–500 nm ( $\epsilon = 3.6\text{--}4.4 \times 10^3$  dm<sup>3</sup> mol<sup>−1</sup> cm<sup>−1</sup>) in acetonitrile solution (Fig. 4a). With reference to previous spectroscopic works on Schiff base platinum(II) complexes,<sup>5</sup> the absorption bands at  $\lambda < 350$  nm are assigned to the intraligand (IL) transition of pyrro-2-yl Schiff base ligands, while the absorption bands at 350–410 nm and 410–500 nm are tentatively ascribed to the platinum(II)-perturbed, ligand-centered <sup>1</sup>( $\pi \rightarrow \pi^*$ ) transition of the Schiff base ligand and <sup>1</sup>[Pt(5d)  $\rightarrow \pi^*$ (Schiff base)] MLCT character, respectively. The absorption spectra are not distinguishable from each other, however,

**Figure 2.** Crystal structures and crystal packing diagrams of (*R,R*)-**PtL** and (*S,S*)-**PtL** with atom numbering.

**Table 2**Parameters for intermolecular C–H⋯Pt(II) interaction in (R,R)-**PtL**, (S,S)-**PtL**, and Tr-**PtL**.

complex	C–H⋯Pt	<i>d</i> /Å <sup>a</sup>	<i>D</i> /Å <sup>b</sup>	<i>θ</i> /° <sup>c</sup>
(R,R)- <b>PtL</b>	C11A–H11A⋯Pt3B	3.066	4.016	167.1
	C6CA–H6CA⋯Pt3B	2.988	3.836	145.5
	C43B–H43B⋯Pt1B	2.910	3.760	145.6
(S,S)- <b>PtL</b>	C42B–H42D⋯Pt2C	3.071	4.073	155.0
	C27C–H27C⋯Pt3C	2.804	3.684	149.7
	C43C–H43C⋯Pt2C	2.957	3.824	148.0
Tr- <b>PtL</b>	C11B–H11B⋯Pt1D	3.065	3.918	146.2
	C11D–H11D⋯Pt1B	3.065	3.918	146.2

<sup>a</sup> For H⋯Pt distance.<sup>b</sup> For C–Pt distance.<sup>c</sup> For C–H⋯Pt(II) angle.

the optically pure enantiomers of (R,R)-**PtL** ( $[\alpha]_D^{20} -1119$  (c 0.0022, CH<sub>2</sub>Cl<sub>2</sub>)) and (S,S)-**PtL** ( $[\alpha]_D^{20} +1120$  (c 0.0023, CH<sub>2</sub>Cl<sub>2</sub>)) show near mirror image behaviors in the circular dichroism (CD) spectra (Fig. 4b). Correlated with the observed CD spectra, the absolute configuration of (R,R)-**PtL** and (S,S)-**PtL** can be subsequently assigned to  $\Delta$  and  $\Lambda$ , respectively, in terms of the definition of IUPAC nomenclature<sup>13a</sup> and the reference method,<sup>13b,c</sup> which is in line with their crystal analysis.

Complexes of (R,R)-**PtL** and (S,S)-**PtL** display a well-resolved structural emission at 560 nm and a shoulder at 610 nm in acetonitrile solution at room temperature (Fig. 4). The emission lifetime of 2.1  $\mu$ s and luminescent quantum yield of 0.008 are comparable to the related Schiff base platinum(II) complexes.<sup>5</sup> The large Stokes shift and lifetime in the microsecond range for the photoluminescence of (R,R)-**PtL** and (S,S)-**PtL** suggest that the emission originates from a triplet parentage. An excimeric emission assignment is not preferred because the emission

maximum is independent on the concentration of complexes of (R,R)-**PtL** and (S,S)-**PtL** in acetonitrile solution (Fig. 4c). The emissions of (R,R)-**PtL** and (S,S)-**PtL** in the solid state at room temperature are also structured with the vibronic progressions of about 1300 cm<sup>−1</sup> (Fig. 4d). Considering the intermolecular metal⋯metal contacts (4.058 Å at Pt3B–Pt1B and 6.057 Å at Pt1A–Pt3B) of (R,R)-**PtL** and (S,S)-**PtL** are beyond the range of intermolecular metal⋯metal distance (3.09–3.50 Å), normally observed in monomeric Pt(II) extended linear-chain structures,<sup>1–4</sup> the distinct *M* and *P* helices' formation driven by intermolecular C–H⋯Pt(II) interaction results in the typical <sup>3</sup>( $\pi\pi^*$ ) excited state with some mixing of the Pt(II) metal character observed both in the solution and in the solid state. This is in contrast to the metal–metal and/or excimeric interaction-directed unusual color and wavelength-dependent emissions of mononuclear platinum(II) complexes obtained in concentrated solutions and/or in the solid states.

### 3. Conclusions

In summary, (R,R)-(–)- and (S,S)-(+)-1,2-bis(pyrrol-2-ylmethyl-eneamino)cyclohexane platinum(II) complexes of (R,R)-**PtL** and (S,S)-**PtL** have been achieved in high yields. The intriguing intermolecular C–H⋯Pt(II) interaction shows a considerable strength and directionality for controlling the self-assembly of (R,R)-**PtL** and (S,S)-**PtL**, leading to *M* and *P* helical supramolecular architectures in crystal lattices. Unlike the metal–metal and/or excimeric interaction-directed unusual color and wavelength-dependent emissions of platinum(II) complexes, the metal-directed interaction is responsible for the <sup>3</sup>( $\pi\pi^*$ ) vibronic emission with some mixing of the Pt(II) metal character observed in solution and in the solid state at room temperature. The unique properties of (R,R)-**PtL** and (S,S)-**PtL** make these complexes of interest for application as phosphorescence emitters in OLEDs and as photocatalysts for solar energy conversion.

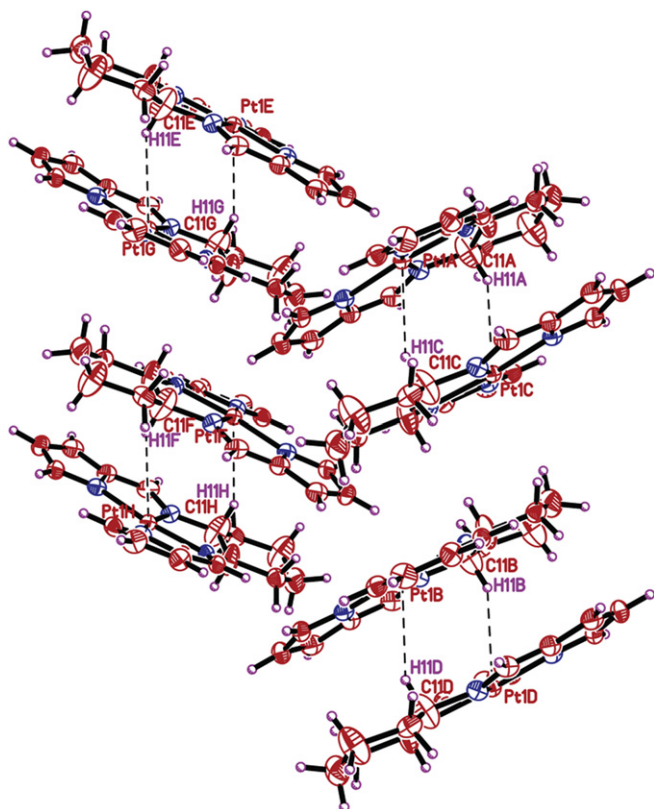
## 4. Experimental section

### 4.1. Materials and instrumentation

All reagents for synthesis were of analytical grade and used as-received. The ligands of (R,R)-**H<sub>2</sub>L** and (S,S)-**H<sub>2</sub>L** were synthesized according to the literature method.<sup>10e</sup> The solvents for spectroscopic measurements were purified according to the literature method.<sup>14</sup> Melting points were determined on a Yanaco MP-500 micro-melting point apparatus. NMR spectra were recorded on a Bruker Avance dpx 400 MHz instruments using TMS as an internal standard. Mass spectra were obtained on Bruker APEX II spectrometers. Elemental analyses were performed on a FLASH EA1112 elemental analyzer. The UV–vis absorption spectra were recorded using a Shimadzu 1601 spectrophotometer. HPLC were performed using a CHIRALPAK<sup>®</sup> IA column 250×10 mm (L×I.D.). The circular dichroism (CD) spectra were measured with a JASCO J-810 Spectropolarimeter. The values of specific rotation were measured on Perkin Elmer 341LC polarimeter. The photoluminescence spectra were determined on a Hitachi 4500 spectrophotometer. The photoluminescence lifetimes were carried out on Edinburgh LP 920. Ru(bpy)<sub>3</sub>(PF<sub>6</sub>)<sub>2</sub> was used as a reference standard for photoluminescence quantum efficiency determination (0.062 in argon saturated acetonitrile).

#### 4.1.1. (R,R)-(–)-1,2-Bis(pyrrol-2-ylmethyleneamino)cyclohexane platinum(II) complex ((R,R)-**PtL**)

Sodium acetate (2 mmol) was suspended in a solution of (R,R)-**H<sub>2</sub>L** (1 mmol) in freshly distilled DMF (15 mL). K<sub>2</sub>PtCl<sub>4</sub> (1 mmol) in

**Figure 3.** Crystal packing diagram of Tr-**PtL**.



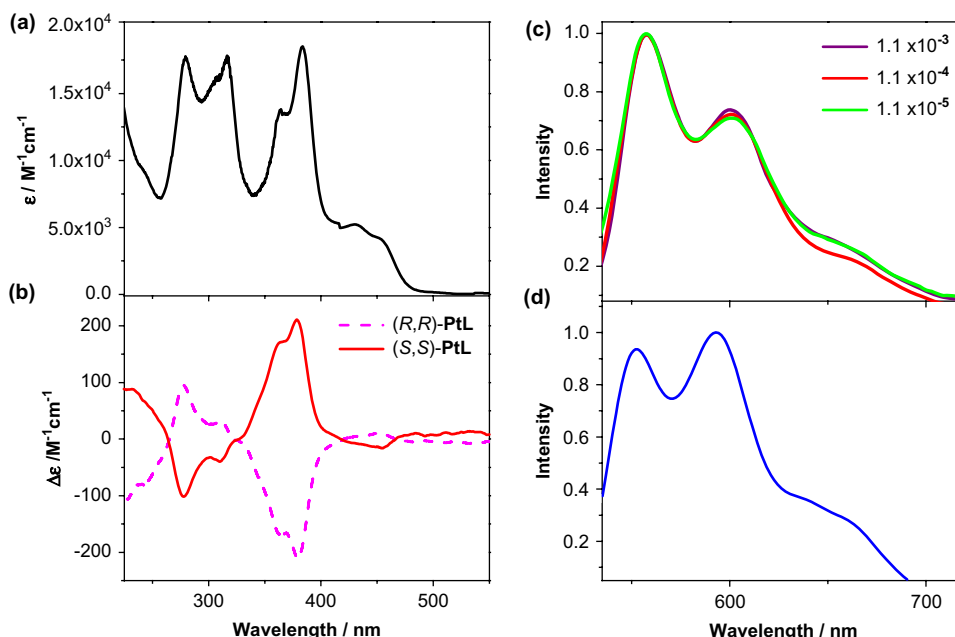


**Figure 4.** The absorption spectra (a) and circular dichroism spectra (b) of (R,R)-PtL, (S,S)-PtL, and Tr-PtL in acetonitrile. The emission spectra of (R,R)-PtL in acetonitrile solution at ambient temperature (c). The solid state emission spectrum of (R,R)-PtL, (S,S)-PtL at ambient temperature (d).

DMSO (5 mL) was introduced dropwise to the suspension at 80 °C. The solution was heated for 4 h. Distilled water (50 mL) was added to the solution upon cooling. The orange precipitate was collected by suction filtration, washed twice with distilled water, and dried under vacuum. Further recrystallization from dichloromethane-methanol gave the expected products of complex (R,R)-PtL. Yield: 180 mg, 79%. Mp: 256 °C (dec),  $[\alpha]_D^{20} -1119$  (c 0.0022,  $\text{CH}_2\text{Cl}_2$ ).  $^1\text{H}$  NMR (400 MHz,  $\text{CDCl}_3$ ,  $\delta$  ppm): 1.32–1.46 (m, 4H), 1.84 (d, 2H), 2.38 (d, 2H), 3.95–3.97 (m, 2H), 6.32 (dd,  $J=4.0$  and 2.1 Hz, 2H), 6.75 (dd,  $J=1.8$  and 4.0 Hz, 2H), 7.09 (s, 2H), 7.61 (s, 2H).  $^{13}\text{C}$  NMR (100 MHz,  $\text{CDCl}_3$ ,  $\delta$  ppm): 24.2, 27.0, 74.2, 110.6, 118.5, 137.2, 145.2, 151.8. HRMS (FAB) Calcd for  $\text{C}_{16}\text{H}_{18}\text{N}_4\text{Pt}$  (M) $^{+}$ : 460.1153; found: 460.1133. Anal. Calcd (%) for  $\text{C}_{16}\text{H}_{18}\text{N}_4\text{Pt}$ : C, 41.65; H, 3.93; N, 12.14. Found: C, 41.43; H, 3.93; N, 11.99.

#### 4.1.2. (S,S)-(+)-1,2-Bis(pyrrol-2-ylmethyleneamino)cyclohexane platinum(II) complex ((S,S)-PtL)

The synthetic procedure was similar to (R,R)-PtL except the ligand (S,S)-H<sub>2</sub>L was used in place of (R,R)-H<sub>2</sub>L. Yield: 178 mg, 78%.  $[\alpha]_D^{20} +1120$  (c 0.0023,  $\text{CH}_2\text{Cl}_2$ ). Mp: 260 °C (dec).  $^1\text{H}$  NMR (400 MHz,  $\text{CDCl}_3$ ,  $\delta$  ppm): 1.32–1.46 (m, 4H), 1.84 (d, 2H), 2.38 (d, 2H), 3.95–3.97 (m, 2H), 6.32 (dd,  $J=4.0$  and 2.1 Hz, 2H), 6.75 (dd,  $J=1.8$  and 4.0 Hz, 2H), 7.09 (s, 2H), 7.61 (s, 2H).  $^{13}\text{C}$  NMR (100 MHz,  $\text{CDCl}_3$ ,  $\delta$  ppm): 24.2, 27.1, 74.1, 110.5, 118.4, 137.1, 145.2, 151.8. HRMS (FAB) Calcd for  $\text{C}_{16}\text{H}_{18}\text{N}_4\text{Pt}$  (M) $^{+}$ : 460.1153; found: 460.1135. Anal. Calcd (%) for  $\text{C}_{16}\text{H}_{18}\text{N}_4\text{Pt} \cdot 0.2\text{CH}_2\text{Cl}_2$ : C, 40.67; H, 3.88; N, 11.71. Found: C, 40.76; H, 3.80; N, 11.69.

#### 4.1.3. trans-(±)-1,2-Bis(pyrrol-2-ylmethyleneamino)cyclohexane platinum(II) complex (Tr-PtL)

The synthetic procedure was similar to (R,R)-PtL except the ligand Tr-H<sub>2</sub>L was used in place of (R,R)-H<sub>2</sub>L. Yield: 184 mg, 80%. Mp: 252 °C (dec).  $^1\text{H}$  NMR (400 MHz,  $\text{CDCl}_3$ ,  $\delta$  ppm): 1.32–1.46 (m, 4H), 1.84 (d, 2H), 2.38 (d, 2H), 3.95–3.97 (m, 2H), 6.32 (dd,  $J=4.0$  and 2.1 Hz, 2H), 6.75 (dd,  $J=1.8$  and 4.0 Hz, 2H), 7.09 (s, 2H), 7.61 (s, 2H).  $^{13}\text{C}$  NMR (100 MHz,  $\text{CDCl}_3$ ,  $\delta$  ppm): 24.2, 27.0, 74.2, 110.5, 118.4, 137.2, 145.2, 151.8. HRMS (FAB) Calcd for  $\text{C}_{16}\text{H}_{18}\text{N}_4\text{Pt}$  (M) $^{+}$ : 460.1153; found: 460.1130. Anal. Calcd (%) for  $\text{C}_{16}\text{H}_{18}\text{N}_4\text{Pt} \cdot 0.5\text{CH}_3\text{OH}$ : C, 41.51; H, 4.20; N, 11.73. Found: C, 41.45; H, 3.98; N, 11.54.

## 4.2. X-ray crystallographic studies

The crystals of (R,R)-PtL, (S,S)-PtL, and Tr-PtL suitable for X-ray analysis were obtained by slow evaporation of dichloromethane-methanol (2:1) solution. Accurate unit cell parameters were determined by least-squares fit of  $2\theta$  values, measured for 200 strong reflections, and intensity data sets were measured on a Rigaku Raxis Rapid IP or a Bruker Smart 1000 CCD diffractometer with Mo K $\alpha$  radiation ( $\lambda=0.71073$  Å). The intensities were corrected for Lorentz and polarization effects. All structures were analyzed by direct methods. The non-hydrogen atoms were located in successive difference Fourier synthesis. The final refinement was performed by full-matrix least-squares methods with anisotropic thermal parameters for non-hydrogen atoms on  $F^2$  (SHELXL-97).<sup>15</sup> The hydrogen atoms were added theoretically and treated as riding on the concerted atoms. Crystallographic data for (R,R)-PtL, (S,S)-PtL, and Tr-PtL have been deposited with the Cambridge Crystallographic Data Center as supplementary publication Nos. CCDC 642875, CCDC 642876, and CCDC 642878, respectively.

## Acknowledgements

We are grateful to The National Science Foundation of China (Grants 20333080, 20732007, 20728506, 50473048, and 20672122), The Ministry of Science and Technology of China (Nos. 2004CB719903, 2006CB806105, 2007CB808004, and 2007CB936001), and the Bureau for Basic Research of The Chinese Academy of Sciences for financial support.

## References and notes

- (a) Roundhill, D. M.; Gray, H. B.; Che, C. M. *Acc. Chem. Res.* **1989**, *22*, 55–61; (b) Smith, D. C.; Gray, H. B. *Coord. Chem. Rev.* **1990**, *100*, 169–181; (c) Houlding, V. H.; Miskowski, V. M. *Coord. Chem. Rev.* **1991**, *111*, 145–152; (d) McMillin, D. R.; Moore, J. J. *Coord. Chem. Rev.* **2002**, *229*, 113–121; (e) Yam, V. W. W. *Acc. Chem. Res.* **2002**, *35*, 555–563; (f) Lai, S. W.; Che, C. M. *Top. Curr. Chem.* **2004**, *241*, 27–63.
- (a) Miskowski, V. M.; Houlding, V. H. *Inorg. Chem.* **1989**, *28*, 1529–1533; (b) Kunkely, H.; Vogler, A. J. *Am. Chem. Soc.* **1990**, *112*, 5625–5627; (c) Miskowski, V. M.; Houlding, V. H. *Inorg. Chem.* **1991**, *30*, 4446–4452; (d) Miskowski, V. M.;

- Houlding, V. H.; Che, C. M.; Wang, Y. *Inorg. Chem.* **1993**, 32, 2518–2524; (e) Hambley, T. W. *Inorg. Chem.* **1998**, 37, 3767–3774.
3. (a) Kui, S. C. F.; Chui, S. S. Y.; Che, C. M.; Zhu, N. Y. *J. Am. Chem. Soc.* **2006**, 128, 8297–8309; (b) Wadas, T. J.; Wang, Q. M.; Kim, Y. J.; Flaschenreim, C.; Blanton, T. N.; Eisenberg, R. J. *Am. Chem. Soc.* **2004**, 126, 16841–16849; (c) Chang, S. Y.; Kavitha, J.; Li, S. W.; Hsu, C. S.; Chi, Y.; Yeh, Y. S.; Chou, P. T.; Lee, G. H.; Carty, A. J.; Tao, Y. T.; Chien, C. H. *Inorg. Chem.* **2006**, 45, 137–146; (d) Matsumoto, K.; Arai, S.; Ochiai, M.; Chen, W.; Nakata, A.; Nakai, H.; Kinoshita, S. *Inorg. Chem.* **2005**, 44, 8552–8560.
4. (a) Gliemann, G.; Yersin, H. *Struct. Bonding* **1985**, 62, 87–153; (b) Goshe, A. J.; Steele, I. M.; Bosnich, B. J. *Am. Chem. Soc.* **2003**, 125, 444–451; (c) Lu, W.; Chan, M. C. W.; Zhu, N.; Che, C. M.; Li, C.; Hui, Z. *J. Am. Chem. Soc.* **2004**, 126, 7639–7651; (d) Ma, B.; Li, J.; Djurovich, P. I.; Yousufuddin, M.; Bau, R.; Thompson, M. E. *J. Am. Chem. Soc.* **2005**, 127, 28–29.
5. (a) Lin, Y. Y.; Chan, S. C.; Chan, M. C. W.; Hou, Y. J.; Zhu, N. Y.; Che, C. M.; Liu, Y.; Wang, Y. *Chem.—Eur. J.* **2003**, 9, 1264–1272; (b) Che, C. M.; Chan, S. C.; Xiang, H. F.; Chan, M. C. W.; Liu, Y.; Wang, Y. *Chem. Commun.* **2004**, 1484–1485; (c) Xiang, H. F.; Chan, S. C.; Wu, K. K. Y.; Chen, C. M.; Lai, P. T. *Chem. Commun.* **2005**, 1408–1410; (d) Sawodny, W.; Thewalt, U.; Potthoff, E.; Oehl, R. *Acta. Crystallogr.* **1999**, C55, 2060–2061.
6. (a) Wu, L.-Z.; Cheung, T. C.; Che, C. M.; Cheung, K. K.; Lam, M. H. W. *Chem. Commun.* **1998**, 1127–1128; (b) Yang, Q. Z.; Wu, L.-Z.; Wu, Z. X.; Zhang, L. P.; Tung, C. H. *Inorg. Chem.* **2002**, 41, 5653–5655; (c) Sun, W.; Wu, Z. X.; Yang, Q. Z.; Wu, L.-Z.; Tung, C. H. *Appl. Phys. Lett.* **2003**, 82, 850–852; (d) Yang, Q. Z.; Wu, L.-Z.; Zhang, H.; Chen, B.; Wu, Z. X.; Zhang, L. P.; Tung, C. H. *Inorg. Chem.* **2004**, 43, 5195–5197; (e) Yang, Q. Z.; Tong, Q. X.; Wu, L.-Z.; Wu, Z. X.; Zhang, L. P.; Tung, C. H. *Eur. J. Inorg. Chem.* **2004**, 1948–1954; (f) Han, X.; Wu, L.-Z.; Si, G.; Pan, J.; Yang, Q. Z.; Zhang, L. P.; Tung, C. H. *Chem.—Eur. J.* **2007**, 13, 1231–1239.
7. (a) Li, X. H.; Wu, L.-Z.; Zhang, L. P.; Tung, C. H.; Che, C. M. *Chem. Commun.* **2001**, 2280–2281; (b) Zhang, D.; Wu, L.-Z.; Yang, Q. Z.; Li, X. H.; Zhang, L. P.; Tung, C. H. *Org. Lett.* **2003**, 5, 3221–3224; (c) Yang, Y.; Zhang, D.; Wu, L.-Z.; Chen, B.; Zhang, L. P.; Tung, C. H. *J. Org. Chem.* **2004**, 69, 4788–4791; (d) Zhang, D.; Wu, L.-Z.; Zhou, L.; Han, X.; Yang, Q. Z.; Zhang, L. P.; Tung, C. H. *J. Am. Chem. Soc.* **2004**, 126, 3440–3441; (e) Feng, K.; Zhang, R. Y.; Wu, L.-Z.; Tu, B.; Peng, M. L.; Zhang, L. P.; Zhao, D.; Tung, C. H. *J. Am. Chem. Soc.* **2006**, 128, 14685–14690; (f) Feng, K.; Wu, L.-Z.; Zhang, L. P.; Tung, C. H. *Tetrahedron* **2007**, 63, 4907–4911.
8. (a) Braga, D.; Grepioni, F.; Tedesco, E. *Organometallics* **1997**, 16, 1846–1856; (b) Desiraju, G. R.; Steiner, T. *The Weak Hydrogen Bond in Structural Chemistry and Biology*; Oxford University Press: Oxford, 1999; (c) Jeffrey, G. A.; Saenger, W. *Hydrogen Bonding in Biological Structures*; Springer: Berlin, 1991; (d) Zhang, J. Q.; Huang, F. H.; Li, N.; Wang, H.; Gibson, H. W.; Gantzel, P.; Rheingold, A. L. *J. Org. Chem.* **2007**, 72, 8935–8938.
9. (a) Brammer, L. *Dalton Trans.* **2003**, 3145–3157; (b) Calhorda, M. J. *Chem. Commun.* **2000**, 801–809.
10. (a) Yang, L. Y.; Chen, Q. Q.; Li, Y.; Xiong, S. X.; Li, G. P.; Ma, J. S. *Eur. J. Inorg. Chem.* **2004**, 1478–1487; (b) Alyea, E. C.; Ferguson, G.; Kannan, S. *Chem. Commun.* **1998**, 345–346; (c) Mukhopadhyay, A.; Pal, S. *Eur. J. Inorg. Chem.* **2006**, 4879–4887; (d) Shan, X.-F.; Wu, L.-Z.; Zhang, L.-P.; Tung, C.-H. *Chin. Sci. Bull.* **2007**, 52, 1581–1584; (e) Shan, X.-F.; Wu, L.-Z.; Liu, X.-Y.; Zhang, L.-P.; Tung, C.-H. *Eur. J. Inorg. Chem.* **2007**, 3315–3319 and references therein; (f) Wang, Y. B.; Fu, H. B.; Shen, F.; Sheng, X. H.; Peng, A. D.; Gu, Z. J.; Ma, H. W.; Ma, J. S.; Yao, J. N. *Inorg. Chem.* **2007**, 46, 3548–3556.
11. (a) Wu, Z. K.; Chen, Q. Q.; Xiong, S. X.; Xin, B.; Zhao, Z. W.; Jiang, L. J.; Ma, J. S. *Angew. Chem., Int. Ed.* **2003**, 42, 3271–3274; (b) Yang, L. Y.; Chen, Q. Q.; Yang, G. Q.; Ma, J. S. *Tetrahedron* **2003**, 59, 10037–10041; (c) Bacchi, A.; Carcelli, M.; Gabba, L.; Ianelli, S.; Pelagatti, P.; Pelizzi, G.; Rogolino, D. *Inorg. Chim. Acta* **2003**, 342, 229–235; (d) Wu, Z. K.; Yang, G. Q.; Chen, Q. Q.; Liu, J. G.; Yang, S. Y.; Ma, J. S. *Inorg. Chem. Commun.* **2004**, 7, 249–252.
12. (a) Mizutani, T.; Yagi, S.; Morinaga, T.; Nomura, T.; Takagishi, T.; Kitagawa, S.; Ogoishi, H. *J. Am. Chem. Soc.* **1999**, 121, 754–759; (b) Wood, T. E.; Dalglish, N. D.; Power, E. D.; Thompson, A.; Chen, X. M.; Okamoto, Y. *J. Am. Chem. Soc.* **2005**, 127, 5740–5741; (c) Wood, T. E.; Ross, A. C.; Dalglish, N. D.; Power, E. D.; Thompson, A.; Chen, X. M.; Okamoto, Y. *J. Org. Chem.* **2005**, 70, 9967–9974; (d) Al-Sheikh-Ali, A.; Cameron, K. S.; Cameron, T. S.; Robertson, K. N.; Thompson, A. *Org. Lett.* **2005**, 7, 4773–4775.
13. (a) Fujita, J.; Shimura, Y. *Spectroscopy and Structure of Metal Chelate Compounds*; Nakamoto, K., McCarthy, P. J., Eds.; John Wiley and Sons: New York, NY, 1968; Chapter 5 and references therein; (b) Downing, R. S.; Urbach, F. L. *J. Am. Chem. Soc.* **1970**, 92, 5861–5865; (c) Wang, F.; Zhang, H.; Li, L.; Hao, H. Q.; Wang, X. Y.; Chen, J. G. *Tetrahedron: Asymmetry* **2006**, 17, 2059–2063.
14. Perrin, D. D.; Armarego, W. L. F. *Purification of Laboratory Chemicals*, 3rd ed.; Pergamon: Oxford, 1988.
15. Sheldrick, G. M. *SHELX 97, Programs for Crystals Structure Analysis*; University of Göttingen: Göttingen, Germany, 1997.